

# Journal Pre-proof

Endocardial electro-anatomic mapping in healthy horses: Normal sinus impulse propagation in the left and right atrium and the ventricles

G. Van Steenkiste, L. Vera, A. Decloedt, S. Schauvliege, T. Boussy, G. van Loon



PII: S1090-0233(20)30029-0

DOI: <https://doi.org/10.1016/j.tvjl.2020.105452>

Reference: YTVJL 105452

To appear in: *The Veterinary Journal*

Accepted Date: 26 March 2020

Please cite this article as: { doi: <https://doi.org/>

This is a PDF file of an article that has undergone enhancements after acceptance, such as the addition of a cover page and metadata, and formatting for readability, but it is not yet the definitive version of record. This version will undergo additional copyediting, typesetting and review before it is published in its final form, but we are providing this version to give early visibility of the article. Please note that, during the production process, errors may be discovered which could affect the content, and all legal disclaimers that apply to the journal pertain.

© 2019 Published by Elsevier.

## Original Article

### Endocardial electro-anatomic mapping in healthy horses: Normal sinus impulse propagation in the left and right atrium and the ventricles

G. Van Steenkiste <sup>a,\*</sup>, L. Vera <sup>a</sup>, A. Decloedt <sup>a</sup>, S. Schauvliege <sup>b</sup>, T. Boussy <sup>c</sup>, G. van Loon <sup>a</sup>

<sup>a</sup> *Equine Cardioteam Ghent University, Department of Large Animal Internal Medicine, Faculty of Veterinary Medicine, Ghent University, Merelbeke, Belgium*

<sup>b</sup> *Department of Surgery and Anesthesiology of Domestic Animals, Faculty of Veterinary Medicine, Ghent University, Merelbeke, Belgium*

<sup>c</sup> *Department of Cardiology, AZ Groeninge, Kortrijk, Belgium*

\* Corresponding author. Tel.: +32 9 264 75 82.

*E-mail address:* [Glenn.VanSteenkiste@ugent.be](mailto:Glenn.VanSteenkiste@ugent.be) (G. Van Steenkiste).

#### Highlights

- This is the first complete 3D electro-anatomical activation map in horses.
- The right and left atrial depolarisation showed individual P wave deflections.
- The interatrial activation pattern supported the presence of Bachmann bundle.
- The complete ventricular depolarisation contributed to the ECG QRS complex.
- Electrically active tissue could be found in all pulmonary veins.

#### Abstract

Understanding the depolarisation pattern of the equine heart under normal physiologic conditions, and its relationship to the surface electrocardiogram (ECG), is of uppermost importance before any further research can be done about the pathophysiology of complex arrhythmias. In the present study, a 3D electro-anatomical mapping system was used to evaluate the qualitative and quantitative depolarisation patterns and correlation to the surface ECG of both the atrial and ventricular endocardium in seven healthy horses in sinus rhythm under general anaesthesia. Bipolar activation maps of the endocardium were analysed.

The first atrial activation was located at the height of the terminal crest. Only one interatrial conduction pathway was recognised. The first and second P wave deflections represent the right and left atrial depolarisation, respectively. Bundle of His electrograms could be recorded in 5/7 horses. Left ventricular activation started at the mid septum and right ventricular activation started apically from the supraventricular crest. This was followed by separate depolarisations at the height of the mid free wall. Further ventricular depolarisation occurred in an explosive pattern. Electrically active tissue could be found in all pulmonary veins. In contrast to findings of previous studies, all parts of the ventricular depolarisation contributed to the surface ECG QRS complex. This study provides a reference for the normal sinus impulse endocardial propagation pattern and for conduction velocities in equine atria and ventricles.

*Keywords:* Arrhythmia; Atrial conduction; Electrocardiogram; Electrophysiology; Ventricular Conduction

## **Introduction**

Normal endocardial atrial and ventricular propagation has been studied in humans and dogs (Cassidy et al., 1984; Derakhchan et al., 2001; De Ponti et al., 2002). In horses, the atrial and ventricular propagation has only been described using invasive epicardial or transmural electrophysiology studies, but not yet under physiological conditions (Hamlin et al., 1970; Muylle, 1975; Muylle and Oyaert, 1975a, 1975b, 1977). Former studies suggested that the surface ECG QRS complex mainly represents the apical third or the basal third of the interventricular septum, thus limiting the diagnostic value of the ECG for ventricular pathologies such as the origin of ventricular ectopy and dilation. (Hamlin and Smith, 1965; Muylle and Oyaert, 1975a, 1975b). However, other authors have reported that certain characteristics of the

surface ECG may indicate the origin of ventricular and atrial arrhythmias (Hamlin et al., 1964; Pfister et al., 1984; Glenn Van Steenkiste et al., 2019a, 2019b). Some authors suggested that the surface ECG could be used for the assessment of ventricular and atrial dilation (Hamlin and Smith, 1965; Muylle and Oyaert, 1971; Holmes, 1976; Hesselkilde et al., 2016).

In order to unravel the pathophysiology of complex arrhythmias such as atrial tachycardia, the normal depolarisation pattern of the equine heart should first be understood. Recently 3D electro-anatomical mapping of the cardiac activation pattern has been proven to be feasible in adult horses using the Rhythmia mapping system (Boston Scientific; Van Steenkiste et al., 2020). This electro-anatomical mapping system rapidly obtains high resolution electro-anatomical activation maps with automatic annotation of endocardial electrograms (EGMs). The system tracks the 3D location of the catheter in the heart using impedance sensing or using a magnetic sensor in the catheter in combination with an external magnetic field generator. Using this technique, the endocardial depolarisation of the atria and ventricles can be visualised on a 3D anatomical map of the heart.

In the present study this electro-anatomical mapping system was used to evaluate both the qualitative and quantitative depolarisation patterns of both the atrial and ventricular endocardium in seven healthy horses in sinus rhythm under general anaesthesia. The atrial and ventricular depolarisation patterns were also correlated to the morphology of the P wave and QRS complex on the surface ECG, respectively.

## **Materials and methods**

### *Horses*

This research was approved by the Ethical Committee of the Faculty of Veterinary Medicine, Ghent University (Approval number, EC2016/35; Approval date, 1 June 2016). Seven horses, aged median 11 years (range, 5-20 years), median height at the withers 162 cm (range, 155-165 cm) and median bodyweight 545 kg (range, 444-631 kg) were studied. Horses were included if no murmurs were present on auscultation, serum biochemistry (electrolytes and cardiac troponin I [cTnI]) was within reference values, no structural abnormalities were found on echocardiography and electrocardiography (ECG) showed normal sinus rhythm. The presence of an occasional second-degree AV block on the ECG was allowed. Horses 1 to 4 were owned by the Faculty of Veterinary Medicine. Horses 5 to 7 were donated by their owners for scientific research followed by euthanasia due to orthopaedic problems. Informed consent was obtained from all owners. The mapping procedure of all four cardiac chambers was performed under general anaesthesia as described elsewhere (Van Steenkiste et al., 2020).

#### *Data analysis*

Bipolar activation maps were used for data analysis. The activation maps consisted of a colour coded 3D representation of the endocardial conduction (Figs. 1-3) in which the rainbow colour spectrum displays timing from red (depolarised endocardium) to purple (yet to be depolarised endocardium). Qualitative analysis was performed by describing the propagation wave for every chamber and for the interatrial conduction. Data points were automatically annotated using the maximum deflection of the bipolar signal as the local depolarisation time. Activation maps were evaluated with a projection distance (=maximum interpolation distance between data points) of 10 mm, a minimum voltage threshold of 0.03 mV and time steps of 5 ms. Multiple breakthroughs of the sinus impulse were considered if two or more distinct areas were

activated separately with a clear spatial difference (De Ponti et al., 2002). The location and depolarisation timing relative to the maximum QRS complex amplitude on the surface ECG for the Bundle of His was recorded if the Bundle of His EGM could be identified.

For the quantitative analysis, measurements of the time intervals during the depolarisation wave were done using the probe tool of the mapping software which displayed the earliest depolarisation within a radius of 5 mm of the calliper. Depolarisation timing was calculated relative to the first endocardial atrial or ventricular depolarisation. The average conduction velocity was calculated by measuring the distance between the pre-defined locations, as listed in Table 2, and dividing the distance by the difference in depolarisation time. Relation with the surface ECG was described relative to lead II of the mapping system, which had a modified base-apex electrode configuration with the positive electrode left of the xyphoid and the negative electrode on the dorsal part of the right spine of the scapula (Van Steenkiste et al., 2020). An index of simultaneous depolarisation for the atria (ISA), in order to assess the period of the atrial systolic time interval during which both atria were activated simultaneously, was calculated according to the following equation (De Ponti et al., 2002):

$$ISA = \frac{(PD_{RA} + PD_{LA}) - ASTI}{ASTI}$$

Where  $PD_{RA}$  and  $PD_{LA}$  are the propagation durations (ms) in the RA and LA, respectively, and  $ASTI$  is the atrial systolic time interval (ms). Data are described as mean  $\pm$  standard deviation.

## Results

A mean of  $13593 \pm 9055$ ,  $26576 \pm 16920$ ,  $22517 \pm 19422$  and  $29236 \pm 16633$  EGMs were acquired for the right and left atrium (RA, LA) and right and left ventricle (RV, LV),

respectively. Stable sinus rhythm was present during mapping. Horses 1 to 4 recovered uneventfully; horses 5 to 7 were euthanized after the procedure as scheduled. A complete LA map could not be obtained in horse 1 and therefore these LA data were not used. The relation of the endocardial depolarisation with the surface ECG is described in Table 1. Depolarisation times of each chamber relative to the first endocardial atrial/ventricular depolarisation are listed in Table 2. Conduction velocities for atria and ventricles are listed in Table 3. Fig. 1 shows the atrial and the ventricular activation pattern is shown in Fig. 2.

#### *Sinus impulse propagation in the atria*

The P wave was bifid in all horses, only in horse 7 the positive bifid P wave was preceded by a small negative deflection. The first atrial activation was located at the level of the terminal crest in all horses and thus denoted as the sinus node (SN) area. In four horses the earliest SN area activation was situated ventromedially to the cranial vena cava (CrVC), in one horse ventrally to the CrVC and in horse 1 ventrolaterally to the CrVC (Fig. 3). Horse 7 had two of the earliest SN activation sites: one lateral area which resulted in a biphasic P wave and one medial area which resulted in a monophasic P wave. The medial site had a 50ms shorter PQ interval on the surface ECG compared to the lateral site and was only active at heart rates below 35 beats per minute. For further data-analysis only the biphasic P wave was included. The SN area was horseshoe shaped ventrally to the CrVC, following the terminal crest.

After initial depolarisation of the sinus node area, the main wavefront propagates medially in a caudodorsal direction towards the intervenous tubercle. In the meantime, the depolarisation wavefront also spreads in a radial way from the main wavefront, but at a lower

conduction velocity. After the main wavefront has reached the intervenous tubercle, the wavefront continues to activate the RA in a radial way. The RA depolarisation ends in the caudal vena cava (CaVC). The electro-anatomic delineation, the anatomical line where the electrical activity is below the threshold of 0.03mV, was very irregular in the CaVC in all cases and well delineated for the CrVC in five cases, but also irregular in two horses.

At the onset of LA depolarisation, 2/3rd of the RA is already activated and the depolarisation wavefront has reached the right sided interatrial septum. In the LA, no breakthroughs could be seen at the height of the interatrial septum. All breakthroughs in the LA occurred at the height of the base of ostium III and/or IV at the location of the previously described insertion of the Bachmann bundle (Hamlin et al., 1970). The depolarisation of the LA occurred radially away from the initial breakthrough site in all horses. A different conduction velocity was observed towards the interatrial septum. Depolarisation of the LA terminated at the left lateral free wall.

#### *Sinus impulse propagation in the ventricles*

Bundle of His EGMs could be recorded in 5/7 horses: five recordings were made in the left ventricle and one in the right ventricle. In the LV, the Bundle of His was recorded from the interventricular septum apical to the noncoronary leaflet of the aortic valve. In the RV, the Bundle of His could be located apically to the septal tricuspid leaflet.

Initial depolarisation of the LV occurred at the high septum in one horse, at the high and mid septum in two horses, and at the middle of the septum in three horses. In all horses, separate

depolarisation of the mid free wall at the height of the insertion of the false tendons occurred shortly after or almost simultaneously with the septal depolarisation. After the initial depolarisation of the septum and the free wall, depolarisation continued in an explosive way without a clear depolarisation wavefront.

Almost simultaneously with the LV, depolarisation of the RV initiated at the height of the septal part of the supraventricular crest in 6/7 horses. In one horse, depolarisation started at the mid free wall and a separate simultaneous depolarisation was found in the mid septum apically to the supraventricular crest. In three horses, a separate depolarisation also started simultaneously in the mid free wall apically to the supraventricular crest. In the remaining horses the mid free wall also depolarised as a separate location immediately after the initial depolarisation. Further depolarisation of the RV inflow tract occurred in an explosive way without a clear depolarisation wavefront in five horses, and with a radial spreading wavefront starting from the initial depolarisation locations in two horses. Depolarisation of the RV outflow tract occurred in a radial way starting from the depolarised areas from the inflow tract. The depolarisation of the RV ended at the pulmonary valve.

## **Discussion**

In the past the myocardial activation pattern was studied using invasive epicardial or transmural electrodes, but until now no endocardial studies were done under less invasive circumstances (Hamlin et al., 1970; Muylle, 1975; Muylle and Oyaert, 1975a, 1975b, 1977). Former studies have led to a better electrophysiological understanding of the equine heart but the data may be biased due to the invasive character of the studies, invading the myocardium. Our

study describes the normal depolarisation in the intact horse and correlates the depolarisation pattern with the deflections of the surface ECG. This knowledge is mandatory in order to use the surface ECG for arrhythmia characterisation (origin, mechanism) and for assessing atrial or ventricular dilation (Hesselkilde et al., 2016; Van Steenkiste et al., 2019b).

The anatomical position of the earliest SN activation including the individual variation between horses in this study was identical to what was described in previous electrophysiological and anatomical studies of the SN (Bishop and Cole, 1967; Hamlin et al., 1970; Muylle and Oyaert, 1975a). The initial depolarization of the SN area could be seen on the surface ECG if the SN area was located medially. This is in contradiction with previous results where the initial atrial depolarisation was not visible, which might be due to the difference in surface ECG lead configurations and because of epicardial mapping (Hamlin et al., 1970; Muylle and Oyaert, 1975a). One horse presented with 2 rate-dependent, probably vagally-mediated, SN exit sites which resulted in a different P wave morphology and PQ interval. This implies that such vagally-induced altered P waves may be hard or impossible to differentiate from atrial ectopy based on a single lead of the surface ECG. The rest of the atrial endocardial conduction pattern was similar as was described by epicardial studies, but we recorded a slightly faster endocardial conduction velocity. This is consistent with endo-/epicardial velocity differences seen in dogs (1.2 m/s vs. 1 m/s; Muylle and Oyaert, 1975a; Derakhchan et al., 2001).

The faster conduction of 1.6 m/s from the terminal crest towards the intervenous tubercle also corresponds to previous results in dogs (Goodman et al., 1971). Since no combined epicardial mapping was done in our study, the conduction velocity of the interatrial band

(Bachmann bundle) could not be measured directly (Derakhchan et al., 2001). Based upon the distance between the intervenous tubercle and the location of first depolarisation in the LA, the estimated continuous velocity on the interatrial band was 1.6 m/s. No indications were found for a conduction delay between the right and left atrium as previously described (Hamlin et al., 1970). Despite the fast conduction velocity of the interatrial band, a large part of the RA was already depolarised before the LA started to depolarise which leads to a smaller index of simultaneous activation for the atria compared to man ( $\pm 0.3$  vs. 0.5 in humans), leading to a bifid P wave on the surface ECG (De Ponti et al., 2002). In one horse, the cranial-dorsal part of the LA along the anatomical pathway of the Bachmann bundle showed a pre-excitation-like pattern as previously described (De Ponti et al., 2002), because the depolarisation on the anatomical pathway occurred within 5 ms of the initial depolarisation of the LA, which is also seen in humans. During sinus rhythm, no pathways of interatrial conduction were found besides the Bachmann bundle, contrary to what is seen in dogs and humans (Derakhchan et al., 2001; De Ponti et al., 2002). However, since no mapping was performed during pacing from various locations within the atrium, other interatrial pathways cannot be excluded. Contrary to human medicine, where the inferior vena cava has a sharp delineation and the superior vena cava is irregularly delineated, the CaVC delineation was very irregular in all horses (De Ponti et al., 2002). In human medicine, myocardial sleeves are found at these areas and these provide a possible substrate for ectopy which may initiate atrial arrhythmias such as atrial tachycardia or atrial fibrillation (Goya et al., 2002). The presence of myocardial sleeves in the equine vena cava has not been described histologically yet, but recently it has been reported that atrial tachycardia can originate from the CaVC in horses (Van Steenkiste et al., 2019). Myocardial

sleeves in the pulmonary veins have been histologically demonstrated in horses (Vandecasteele et al., 2018) and our study demonstrates that these sleeves are electrophysiologically active.

For the first time Bundle of His EGMs could be recorded in the equine ventricles. Only one Bundle of His EGM could be recorded in the RV, probably due to the difficult location underneath the septal tricuspid valve leaflet (Bishop and Cole, 1967). This difficult to access location may hamper the standard ‘four-wire’ electrophysiological diagnostic exam in horses which requires, among other locations, a recording of the Bundle of His EGM (Murgatroyd and Krahn, 2003). The Bundle of His EGM in the LV could not be recorded in two horses because it was difficult to keep the mapping catheter stable underneath the aortic valve due to cardiac motion and blood flow.

Variations could be seen in the initial depolarisation site in both the left and right ventricle, mid septum and mid free wall, but in general the first depolarisations and explosive depolarisation are similar as seen in humans and as described in an epicardial study in horses (Durrer et al., 1970; Muylle and Oyaert, 1975b; Cassidy et al., 1984). The three horses with initial high septal depolarisation also had almost simultaneous mid septal depolarisation. The ventricular conduction velocity represented the conduction via the Purkinje fibres rather than the ventricular myocardial cells due to the clearly faster speeds.

Some studies have demonstrated that certain characteristics of the surface ECG may indicate the origin of ventricular arrhythmias (Hamlin et al., 1964; Pfister et al., 1984; Van Steenkiste et al., 2019a, 2019b) and assess dilation (Hamlin and Smith, 1965; Muylle and

Oyaert, 1971; Holmes, 1976; Hesselkilde et al., 2016). However, some of these older studies were inconclusive and it was thought that only the apical or basal part of the septum contributes to the surface ECG QRS complex (Hamlin and Smith, 1965; Muylle and Oyaert, 1975b, 1977). However, our study demonstrates that the entire ventricular depolarisation process is represented in the QRS complex. We therefore suggest that appropriate 12-lead surface ECG recordings may provide much more information regarding the origin of ventricular ectopy and size than what is currently believed.

The current study only included a limited number of animals, but despite this limitation only minimal individual variations in the conduction pattern were encountered. However, not all anatomical variations may be included. There was some variation in the first site of ventricular depolarisation, but because the rapid conduction via the Purkinje system delivered the depolarisation at different areas within a very short timeframe, this did not affect QRS morphology or duration. This is in sharp contrast to a ventricular premature beat that depends on slow myocardial cell-to-cell conduction, resulting in altered QRS morphology and duration. For the quantitative analysis of the conduction velocity, only minor variations were seen in the atria. Large variations were seen in the ventricles, but this is due to the indistinctly defined depolarisation wavefront, which made it difficult to measure the conduction velocity and these measurements should be interpreted as estimates. Concurrent epicardial mapping may improve the understanding of the atrial depolarisation pattern, especially the interatrial conduction. Future studies combining both epi- and endocardial mapping should be performed, including experimental pacing at different locations in order to better understand the interatrial conduction

mechanisms. Finally, remapping at higher heart rates using positive chronotropic therapy could provide a better understanding of conduction mechanisms.

## **Conclusions**

This study provides a reference for the normal endocardial sinus depolarisation pattern and conduction velocities in the equine atria and ventricles. The only interatrial conduction pathway identified was Bachmann bundle. The depolarisation of RA and LA could be identified on the surface ECG as the first and second part of the bifid P wave. Most of the ventricular depolarisation occurred very fast without a clear depolarisation front. Contrary to current knowledge, all regions of the ventricular depolarisation contributed to the QRS complex on the surface ECG. Electrophysiologically active tissue could be found in the caudal vena cava and pulmonary veins in all horses.

## **Conflict of interest statement**

None of the authors of this paper has a financial or personal relationship with other people or organisations that could inappropriately influence or bias the content of the paper.

## **Acknowledgements**

Glenn Van Steenkiste and Lisse Vera are PhD fellows of the Research Foundation Flanders, grant 1S56217N and 1134917N, respectively.

## **Supplementary material**

Supplementary data associated with this article can be found, in the online version, at doi:

...

## References

- Bishop, S.P., Cole, C.R., 1967. Morphology of the specialized conducting tissue in the atria of the equine heart. *The Anatomical Record* 158, 401–415.
- Cassidy, D.M., Vassallo, J.A., Marchlinski, F.E., Buxton, A.E., Untereker, W.J., Josephson, M.E., 1984. Endocardial mapping in humans in sinus rhythm with normal left ventricles: activation patterns and characteristics of electrograms. *Circulation* 70, 37–42.
- De Ponti, R., Ho, S.Y., Salerno-Uriarte, J.A., Tritto, M., Spadacini, G., 2002. Electroanatomic analysis of sinus impulse propagation in normal human atria. *Journal of Cardiovascular Electrophysiology* 13, 1–10.
- Derakhchan, K., Li, D., Courtemanche, M., Smith, B., Brouillette, J., Page, P.L., 2001. Method for simultaneous epicardial and endocardial mapping of in vivo canine heart: Application to atrial conduction properties and arrhythmia mechanisms. *Journal of Cardiovascular Electrophysiology* 12, 548–555.
- Durrer, D., van Dam, R.T., Freud, G.E., Janse, M.J., Meijler, F.L., Arzbaecher, R.C., 1970. Total excitation of the isolated human heart. *Circulation* 41, 899–912.
- Goodman, D., van der Steen, A., van Dam, R., 1971. Endocardial and epicardial activation pathways of the canine right atrium. *American Journal of Physiology* 220, 1–11.
- Goya, M., Ouyang, F., Ernst, S., Volkmer, M., Antz, M., Kuck, K.H., 2002. Electroanatomic mapping and catheter ablation of breakthroughs from the right atrium to the superior vena cava in patients with atrial fibrillation. *Circulation* 106, 1317–1320.
- Hamlin, R.L., Smetzer, D.L., Senta, T., Smith, C.R., 1970. Atrial activation paths and P waves in horses. *American Journal of Physiology* 219, 306–313.
- Hamlin, R.L., Smetzer, D.L., Smith, C.R., 1964. Analysis of QRS complex recorded through a semiorthogonal lead system in the horse. *American Journal of Physiology* 207, 325–33.
- Hamlin, R.L., Smith, C.R., 1965. Categorization of common domestic mammals based upon their ventricular activation process. *Annals of the New York Academy of Sciences*. Sci. 127, 195–203.
- Hesselkilde, E.Z., Carstensen, H., Vandsø Petersen, B., Jespersen, T., Kanters, J.K., Buhl, R., 2016. Is ECG in horses only for dysrhythmia diagnosis? Introducing a new method for 12-lead ECG. *Journal of Veterinary Internal Medicine* 30, 1500–1501.
- Holmes, 1976. Spatial Vector changes during ventricular depolarisation using a semi-orthogonal

- lead system-A study of 190 cases. *Equine Veterinary Journal* 8, 1–16.
- Murgatroyd, F.D., Krahn, A.D., 2003. *Handbook of cardiac electrophysiology*. Remedica, London.
- Muyllé, E., 1975. Experimenteel onderzoek naar het verloop van de depolarisatiegolf in het hart van het paard : De genesis van het electrocardiografisch P- en QRS-complex. 1975.
- Muyllé, E., Oyaert, W., 1977. Equine electrocardiography The genesis of the different configurations of the “QRS” complex. *Zentralblatt für Veterinärmedizin R. A* 24, 762–771.
- Muyllé, E., Oyaert, W., 1975a. Atrial activation pathways and the P Wave in the horse. *Zentralblatt für Veterinärmedizin R. A* 22, 474–484.
- Muyllé, E., Oyaert, W., 1975b. Excitation of the ventricular epicardium in the horse. *Zentralblatt für Veterinärmedizin R. A* 22, 463–473.
- Muyllé, E., Oyaert, W., 1971. Clinical evaluation of cardiac vectors in the horse. *Equine Veterinary Journal* 3, 129–136.
- Pfister, R., Seifert-Alioth, C., Beglinger, R., 1984. Die bestimmung des ursprungsortes ventrikulärer extrasystolen beim pferd. *schweizer arch. für tierheilkd. SAT die Fachzeitschrift für Tierärztinnen und Tierärzte* 165–172.
- Van Steenkiste, G., De Clercq, D., Boussy, T., Vera, L., Schauvliege, S., Decloedt, A., van Loon, G., 2020. Three dimensional ultra-high-density electro-anatomical cardiac mapping in horses: Methodology. *Equine Veterinary Journal*, *In press*.
- Van Steenkiste, G., De Clercq, D., Decloedt, A., Vera, L., van Loon, G., 2019a. A 12-lead electrocardiogram interpretation algorithm to determine the anatomical site of origin of atrial premature depolarizations in horses: Preliminary data. *Equine Veterinary Journal*. 51, 8.
- Van Steenkiste, G., De Clercq, D., Vera, L., van Loon, G., 2019b. Specific 12-lead electrocardiographic characteristics that help to localize the anatomical origin of ventricular ectopy in horses: Preliminary data. *Journal of Veterinary Internal Medicine* 33, 1548.
- Van Steenkiste, G., Duytschaever, M., De Clercq, D., Tavernier, R., Michielsens, A., Decloedt, A., Schauvliege, S., van Loon, G., 2019. First successful radiofrequency ablation of atrial tachycardia in a horse guided by a high density 3D electro-anatomical mapping system (rhythmia). *Journal of Veterinary Internal Medicine* 33, 1547.
- Vandecasteele, T., Van Den Broeck, W., Tay, H., Couck, L., van Loon, G., Cornillie, P., 2018. 3D reconstruction of the porcine and equine pulmonary veins, supplemented with the identification of telocytes in the horse. *Anatomia, Histologia, Embryologia* 47, 145–152.

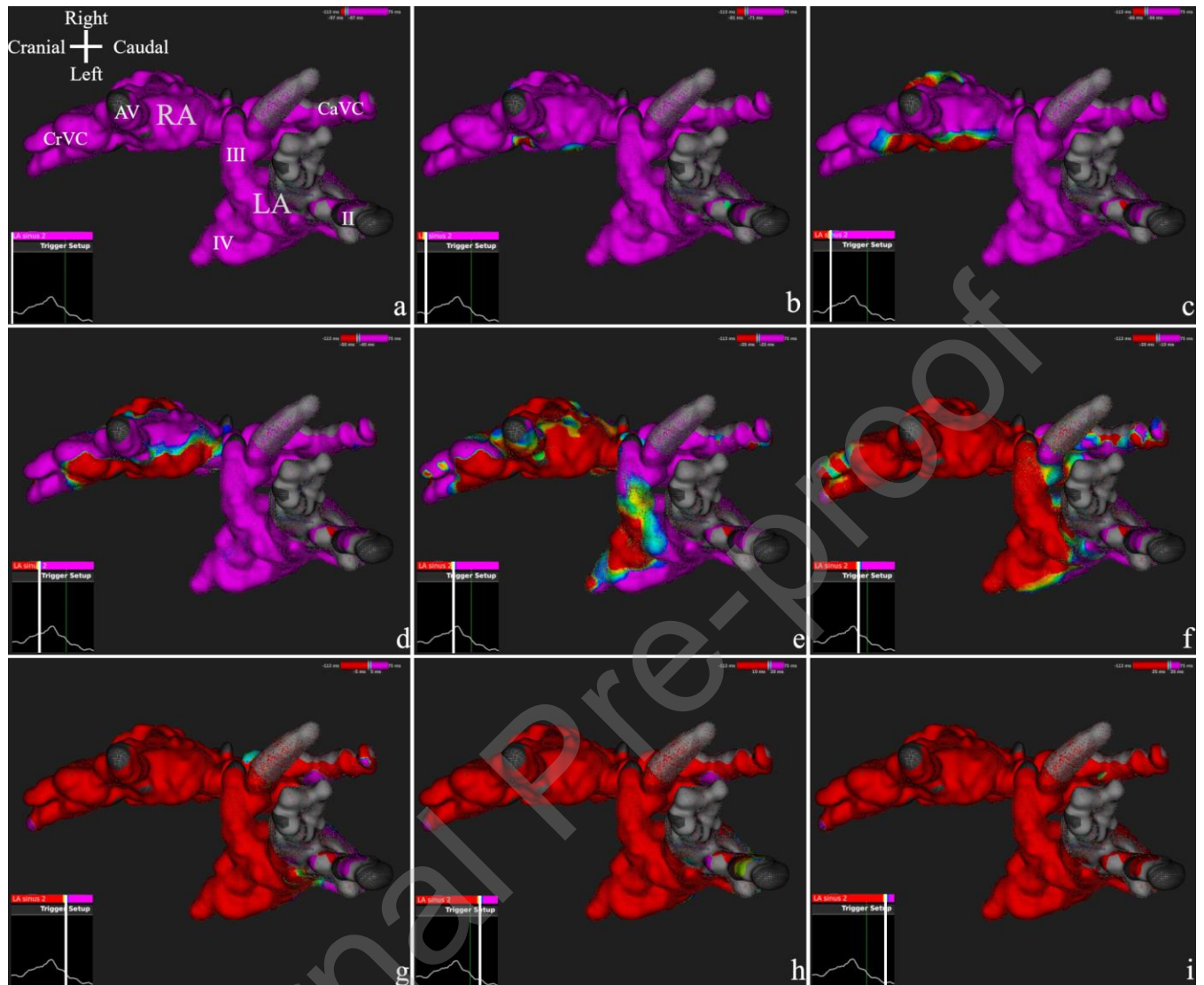


Fig. 1. From subpanel a to i, atrial activation steps from a dorsal view are shown in steps of 10 ms. In the lower left corner of each subpanel, the current timing in relation to lead II of the surface ECG is indicated by a white vertical line. The colour varies following the rainbow colour spectrum from red (earliest depolarisation) to purple (latest depolarisation). A part of the initial and final activation cannot be visualized since it is located apically. In this horse the first atrial activation is located ventromedially. The grey areas indicate a local voltage below the minimal voltage threshold (0.03 mV). AV, azygous vein; CaVC, caudal vena cava; CrVC, cranial vena cava; II,

pulmonary vein ostium II; III, pulmonary vein ostium III; IV, pulmonary vein ostium IV; LA, left atrium; RA, right atrium.

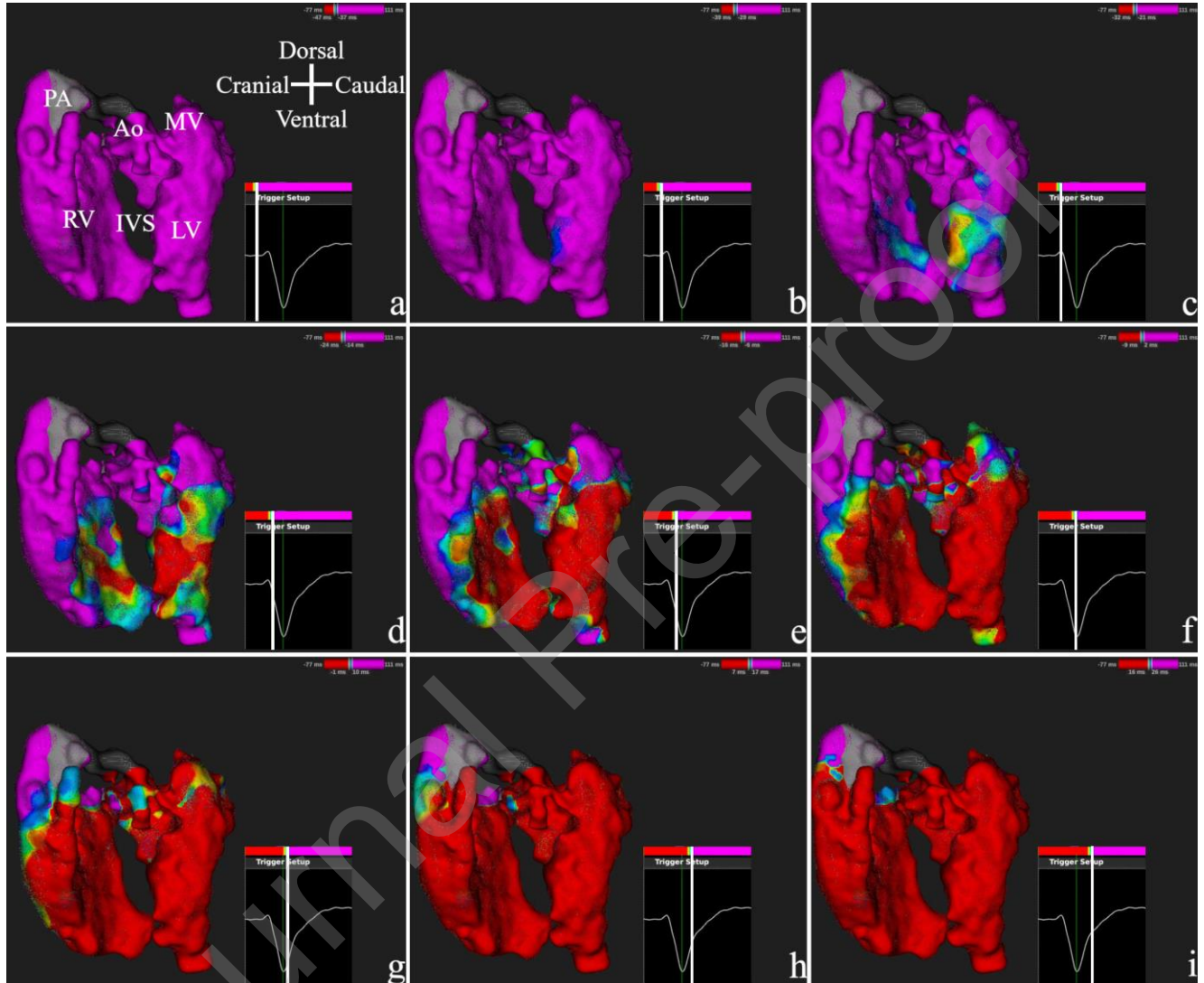


Fig. 2. Activation steps for the ventricles from subpanel a to i with 8 ms between each subpanel. The ventricles are seen from a left view. The ECG trace in the lower right corner represents lead II of the surface ECG. The white vertical line indicates the current time point of that subpanel. The colour varies following the rainbow colour spectrum from red (earliest depolarisation) to purple

(latest depolarisation). Ao, aorta; IVS, interventricular septum; LV, left ventricle; MV, mitral valve; PA, pulmonary artery; RV, right ventricle.

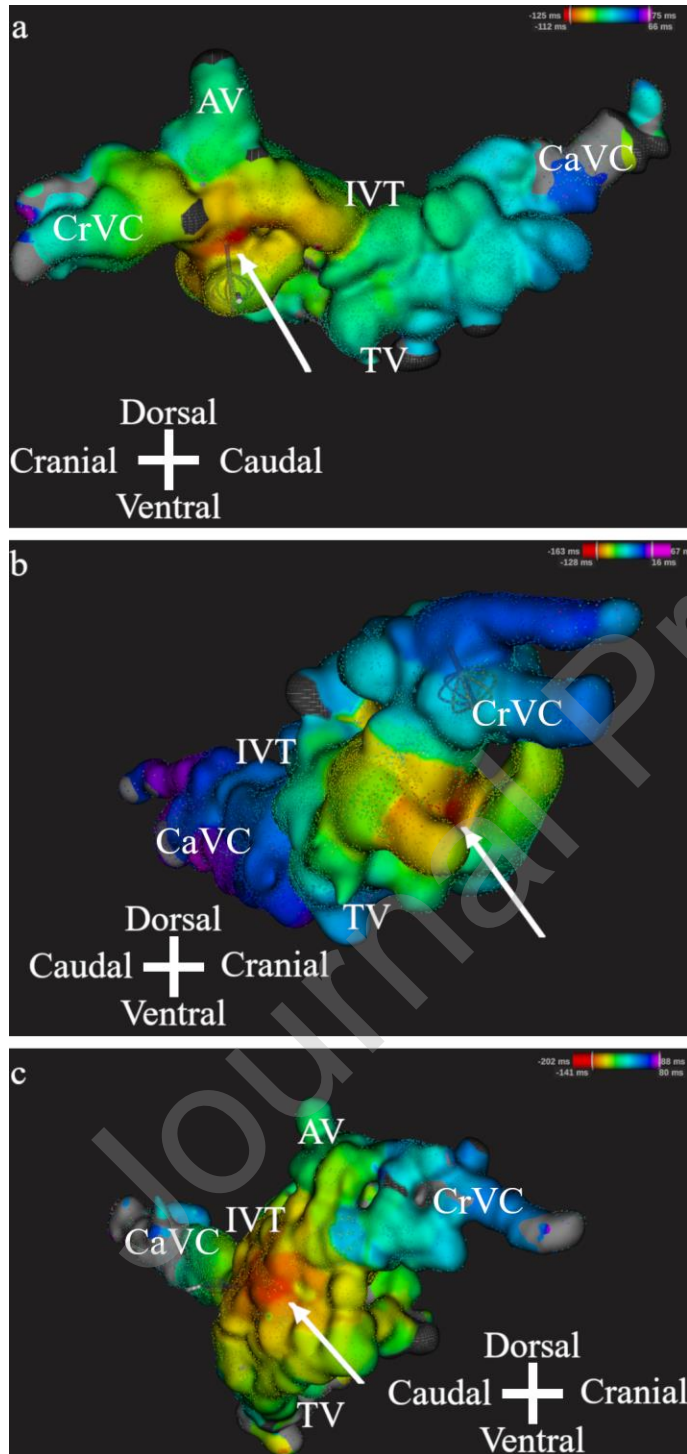


Fig. 3. Areas of first activation of the sinus node area, on static activation maps of the right atrium from three horses. The colour variates following the rainbow colour spectrum from red (earliest depolarisation) to purple (latest depolarisation). The sinus node areas are located medial (panel a), cranial (panel b) and lateral (panel c). AV, azygous vein; CaVC, caudal vena cava; CrVC, cranial vena cava; IVT, intervenous tubercle; TV, tricuspid valve.

**Table 1**

Relation between intracardiac activation and lead II of the mapping system <sup>a</sup>

	Surface ECG morphology	Corresponding activation
P wave	Electrocardiographically silent part of initial atrial depolarisation <sup>b</sup>	24 ms: cranial terminal crest ( <i>n</i> =2) 40 ms: lateral terminal crest ( <i>n</i> =1) 0 ms: medial terminal crest ( <i>n</i> =4)
	Negative initial P wave polarity	Lateral side terminal crest ( <i>n</i> =1)
	Positive initial P wave polarity	Medial and cranial side terminal crest ( <i>n</i> =6)
	Onset 2 <sup>nd</sup> positive P wave deflection	Onset of left atrial depolarisation
QRS complex	Q wave	Depolarisation LV high septum ( <i>n</i> =1)
	R wave	Depolarisation apical 3 <sup>rd</sup> LV septum and RV high septal part of supraventricular crest.
	Between onset QRS and S wave peak	Depolarisation of complete LV with exception of LV high free wall. ( <i>n</i> =7) Depolarisation of RV inflow tract and part of the RV outflow tract ( <i>n</i> =7)

	Depolarisation of the LV high septum ( $n=6$ )
After S wave peak	Depolarisation LV high free wall and RV outflow tract.

---

LV, left ventricle; RV, right ventricle.

<sup>a</sup> Lead II of the mapping system had a modified base-apex electrode configuration with the positive electrode left of the xyphoid and the negative electrode on the dorsal part of the right spine of the scapula.

<sup>b</sup> The durations during which there is atrial activation without electrocardiographic activity on the surface ECG are reported according to each sinus node location.

**Table 2**

Timings (ms) of atrial and ventricular activation.

Chamber	Location	Mean	Standard deviation	Minimum	Maximum
Right atrium ( $n=7$ ) <sup>a</sup>					
	Intervenous tubercle	55	12	38	76
	Free wall at tricuspid valve level	84	22	48	120
	Interatrial septum	93	24	58	137
	Cranial vena cava	115	17	89	141
	Caudal vena cava lateral wall	117	15	98	145
	Caudal vena cava medial wall	127	19	102	163
	Right atrium completely depolarised	139	15	119	168
Left atrium ( $n=6$ ) <sup>a</sup>					
	First depolarization at insertion Bachmann bundle	85	27	53	139
	Base ostium III	92	38	34	142
	Base ostium IV	103	28	73	144
	Base ostium II	117	22	95	151
	Dorsal interatrial septum	121	28	86	158
	Lateral free wall near mitral valve level	150	30	106	191
	Time needed for complete depolarisation of left atrium	68	19	44	101
Both atria ( $n=6$ ) <sup>a</sup>					
	Both atria completely depolarised	156	24	128	191
	Index of simultaneous activation	0.34	0.11	0.16	0.52
Left ventricle ( $n=7$ ) <sup>b</sup>					

Bundle of His apical to aortic valve ( <i>n</i> =5) compared to left ventricular activation	-31 <sup>c</sup>	8	-21	-45 <sup>c</sup>
Mid septum	8	3	0 ( <i>n</i> =5) <sup>d</sup>	11
Lateral mid free wall	11	9	1	26
High septum	15	8	0 ( <i>n</i> =3) <sup>d</sup>	23
Caudal mid free wall	15	9	1	26
Lateral high free wall	26	12	12	43
Caudal high free wall	26	13	8	47
Apex	26	5	17	35
Time needed for complete depolarization of left ventricle	55	16	21	73
Right ventricle ( <i>n</i> =7) <sup>b</sup>				
Bundle of His apical to tricuspid valve ( <i>n</i> =1) compared to right ventricular activation	-51 <sup>c</sup>			
Timing of first activation of right ventricle compared to left ventricle	-3 <sup>c</sup>	8	-16 <sup>c</sup>	7
Septal part of the supraventricular crest	13	11	0 ( <i>n</i> =4)	29
Mid septum	13	7	0 ( <i>n</i> =1)	27
High free wall (outflow tract at the height of tricuspid)	19	8	9	29
Apex	21	5	13	29
Mid free wall	22	6	0 ( <i>n</i> =2)	33
Free wall adjacent to the tricuspid valve	35	19	6	60
Septum adjacent to the tricuspid valve	36	17	11	67
Right ventricular outflow tract adjacent to the pulmonary valve	53	22	27	88

Time needed for complete depolarization of inflow tract	45	15	26	67
Time needed for complete depolarization of right ventricle	58	19	32	88
Both ventricles ( $n=7$ ) <sup>b</sup>				
Complete ventricles depolarized	63	20	38	97

<sup>a</sup> Timings for the atria are relative to the first endocardial activation in the right atrium except if written otherwise.

<sup>b</sup> Timings for the left and right ventricle are relative to the first left and right endocardial activation in the left and right ventricle, respectively.

<sup>c</sup> Negative values indicate activations that occur earlier in time.

<sup>d</sup> One horse had simultaneous initial depolarization of the mid and high left ventricular septum.

**Table 3**

Conduction velocities in m/s within the atria and ventricles

Chamber	Activation type	Mean	Standard deviation	Minimum	Maximum
Right atrium ( <i>n</i> =7)					
	Caudodorsal depolarisation towards intervenous tubercle	1.6	0.3	1.3	2.1
	Radial spreading depolarisation	1.2	0.2	0.9	1.7
	Depolarisation towards cranial vena cava	0.9	0.2	0.6	1.2
Left atrium ( <i>n</i> =6)					
	Radial spreading depolarisation	0.8	0.2	0.3	1.4
	Interatrial septum	0.5	0.2	0.3	0.9
Left ventricle ( <i>n</i> =7)					
	Radial spreading depolarisation <sup>a</sup>	5.8	1.5	1.9	11.6
Right ventricle ( <i>n</i> =7)					
	Radial spreading depolarisation of inflow tract ( <i>n</i> =2)	3.2	0.8	2.1	4.8
	Radial spreading depolarisation of outflow tract	2.8	1.0	0.6	5.0

<sup>a</sup> Estimated value since no clear depolarisation wavefront could be identified

**Supplementary video legends**

Video 1. Three-dimensional electro-anatomical activation map showing the activation sequence of the atria from a dorsal view. For identification of anatomical structures, please refer to Fig. 1.

Video 2. 3D electro-anatomical activation map showing the activation sequence of the ventricles from a left view. For identification of anatomical structures, please refer to Fig. 2.